The melting curve of iron at the pressures of the Earth's core from *ab initio* calculations

D. Alfè*, M. J. Gillan† & G. D. Price*

** Research School of Geological and Geophysical Sciences, Birkbeck College and University College London, Gower Street, London WC1E 6BT, UK*
† Physics and Astronomy Department, University College London, Gower Street, London WC1E 6BT, UK

The solid inner core of the Earth and the liquid outer core consist mainly of iron[1] so that knowledge of the high-pressure thermodynamic properties of iron is important for understanding the Earth's deep interior. An accurate knowledge of the melting properties of iron is particularly important, as the temperature distribution in the core is relatively uncertain[2–4] and a reliable estimate of the melting temperature of iron at the pressure of the inner-core boundary would put a much-needed constraint on core temperatures. Here we used *ab initio* methods to compute the free energies of both solid and liquid iron, and we argue that the resulting theoretical melting curve competes in accuracy with those obtained from high-pressure experiments. Our results give a melting temperature of iron of ~6,700 ± 600 K at the pressure of the inner-core boundary, consistent with some of the experimental measurements. Our entirely *ab initio* methods should also be applicable to many other materials and problems.

The pressure P at the inner-core boundary (ICB) is 330 GPa (ref. 1), and the values for the melting temperature T_m of Fe are needed up to at least this pressure. Static compression measurements of T_m with the diamond anvil cell (DAC) have been made up to ~200 GPa, but even at lower pressures results for T_m disagree by several hundred kelvin (ref. 2). Recent DAC diffraction experiments[3] demonstrate that in the range 60–80 GPa the solid phase from which Fe melts has a hexagonal close-packed ε-phase. Shock experiments are at present the only available method of T_m measurement at higher pressures, but their interpretation is not simple, and there is a scatter of at least 2,000 K in T_m at ICB pressures[2]. Some experiments have been interpreted as indicating a solid phase different from the ε-phase at $P \geqslant 200$ GPa and $T \geqslant 4{,}000$ K, but the evidence is inconclusive[29]. There have also been attempts to obtain the melting curve from parametrized atomistic models for the energetics of iron[4], but the reliability of these models is uncertain.

Parameter-free *ab initio* techniques based on density functional theory (DFT) have recently made enormous strides[5], and for many materials, including transition metals, reliance on parametrized models is now unnecessary. With *ab initio* molecular-dynamics methods[6], this is true for both liquids and solids[5]. Solid iron in all its known crystal structures has been extensively studied with DFT. The accuracy of DFT depends on the approximation used for the electronic exchange-correlation energy, but with the generalized-gradient approximation[7] (GGA) the experimentally observed properties of Fe are very accurately reproduced. These include the equilibrium lattice parameter, bulk modulus, magnetic moment[8] and phonon frequencies[9] of the body-centred cubic α-phase, the volume of the ε-phase as a function of pressure up to core pressures[8,10,11], and the low-temperature coexistence pressure of the α and ε phases[8,10]. Extensive *ab initio* thermodynamics calculations[12,13] for close-packed solid iron under Earth's core conditions have demonstrated impressive agreement with shock data and other experiments. Recently, we reported *ab initio* molecular dynamics simulations[14–16] of liquid Fe and its alloys with sulphur and oxygen, which we used to study the structure and viscosity of these liquids under core conditions.

Here we use the implementation of DFT known as the "projector augmented wave"[17,18]. This is an all-electron technique in the sense that the valence wavefunctions are correctly represented everywhere in space (not 'pseudized' in the atomic-core regions as in pseudopotential methods), and resembles other all-electron methods such as FLAPW (full-potential linear augmented plane wave), used in previous work[8] on solid Fe. It is also similar to the ultrasoft pseudopotential methods used in our earlier work, and, like them, it can be used for dynamical simulations. The present work was done with the Vienna Ab-initio Simulation Package (VASP) code[19] which is extremely robust and stable for simulation of metals. Full technical details will be given elsewhere, but we note that a correct treatment of the 3*p* electrons (and to a much smaller extent the 3*s* electrons) is essential, since these respond significantly to their environment at the pressures of the Earth's core. These effects have been included as in our earlier work on the viscosity of iron[14].

Since Fe melts from the ε-phase in the pressure range immediately above 60 GPa (ref. 3), we focus here on equilibrium between the ε and liquid phases. The condition for two phases to be in thermal equilibrium at a given temperature T and pressure P is that their Gibbs free energies $G(P, T)$ are equal. To determine T_m at any pressure, we calculate G for the solid and liquid phases as a function of T and determine where they are equal. In fact, we calculate the Helmholtz free energy $F(V, T)$ as a function of volume V, and hence obtain the pressure through the relation $P = -(\partial F/\partial V)_T$ and G through its definition $G = F + PV$.

Our calculations of F for solid and liquid Fe build on significant advances in *ab initio* free energy techniques[20,21]. The free energy of the harmonic vibrating solid is conceptually simplest, and is given (per primitive cell) by the standard high-temperature formula: $F = F_{perf} + N_{\mathbf{k}}^{-1}\Sigma_{\mathbf{k}s}\ln(\hbar\omega_{\mathbf{k}s}/k_B T)$ where F_{perf} is the free energy of the rigid perfect lattice and $\omega_{\mathbf{k}s}$ is the frequency of the phonon of branch s at wavevector $\mathbf{k}$. (Here $\hbar$ is Planck's constant divided by 2π, and k_B is Boltzmann's constant.) The sum goes over the $N_{\mathbf{k}}$ wavevectors in the Brillouin zone of the crystal and over the branches s. Note that F_{perf} contains an entropy contribution from thermal excitation of electrons: thermal electronic excitation is included throughout this work for both solid and liquid Fe phases.

To obtain melting properties with useful accuracy, free energies must be calculated with high precision, because the free-energy curves for liquid and solid cross at a shallow angle. It can readily be shown that to obtain T_m with a technical precision of 100 K, non-cancelling errors in G must be reduced below 10 meV. Errors in the rigid-lattice free energy F_{perf} due to basis-set incompleteness and

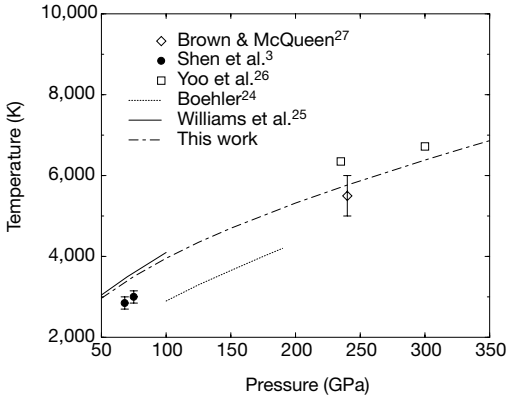

Figure 1 The *ab initio* melting curve of iron compared with experimental results. The dashed curve shows *ab initio* results; solid and dotted curves are interpolations of DAC measurements made by Williams *et al.*[25] and Boehler[24] respectively; the data points due to Shen *et al.*[3] represent a lower bound rather than the melting curve itself; the squares and diamond with error bar are shock data from refs 26 and 27.

Brillouin-zone sampling are readily reduced to a few meV per atom. The frequencies $\omega_{\mathbf{k}s}$ were obtained by diagonalizing the force-constant matrix; this matrix was calculated by our implementation of the small-displacement method described by Kresse *et al.*[22]. The difficulty in calculating the harmonic free energy is that $\omega_{\mathbf{k}s}$ must be accurately converged for wavevectors $\mathbf{k}$ over the whole Brillouin zone. This requires that the free energy is fully converged with respect to the range of the force-constant matrix. To attain the necessary precision we used repeating cells containing 36 atoms, and to show that such cells suffice we went to cells of up to 150 atoms.

To calculate the liquid free energy and the anharmonic contribution to the solid free energy, we use the technique of 'thermodynamic integration', which yields the difference $\Delta F \equiv F - F_{\mathrm{ref}}$ between the free energy of the *ab initio* system and that of a reference system F_{ref}. The basis of the technique[21,23] is that ΔF is the work done on reversibly and isothermally switching from the reference total-energy function U_{ref} to the *ab initio* total energy U. This switching is done by passing through intermediate total-energy functions U_λ given by $U_\lambda = (1-\lambda)U_{\mathrm{ref}} + \lambda U$. It is a standard result that the work done is:

$$\Delta F = \int_0^1 \mathrm{d}\lambda \langle U - U_{\mathrm{ref}} \rangle_\lambda \qquad (1)$$

where the thermal average $\langle U - U_{\mathrm{ref}} \rangle$ is evaluated for the system governed by U_λ. The practical feasibility of calculating *ab initio* free energies of liquids and anharmonic solids depends on finding a reference system for which F_{ref} is readily calculable and the difference $U - U_{\mathrm{ref}}$ is very small.

For the liquid, our threshold precision is only achievable because the *ab initio* energy U is extremely well reproduced by a model U_{ref} consisting of a sum of pair potentials $\phi(r)$, with $\phi(r)$ chosen to be an inverse-power repulsive potential: $\phi(r) = A/r^\alpha$. (Here r is the interatomic distance.) The parameters A and α are adjusted to minimize the strength of the fluctuations $U - U_{\mathrm{ref}}$. We have demonstrated the excellence of this U_{ref} by doing *ab initio* dynamical simulations at 18 different thermodynamic states spanning the (P, T) range of interest, and we find that a single choice of A and α is almost equally good over the whole range. The free energy of the reference model is readily calculated for very large simulated systems, so that size errors are negligible. We then use thermodynamic integration to compute the difference ΔF giving the full *ab initio* free energy. The size errors on ΔF fall below 5 meV for *ab initio* systems of 125 atoms, as we have demonstrated using considerably larger systems; errors due to electronic k-point sampling are readily reduced to the same level. Most of our calculations were actually made using 67 atoms, but corrected for size and k-point errors by doing spot checks on 125 atoms. The inverse-power model is not a good enough reference system for the anharmonic solid, but we find that an extremely good reference system for this case can be obtained by suitably combining the inverse-power and harmonic *ab initio* total energies. Specifically, if U_{IP} is the total energy consisting of the sum of pair potentials $\phi(r)$, and U_{harm} is the harmonic part of the *ab initio* total energy, the reference system we use is $U_{\mathrm{ref}} = c_1 U_{\mathrm{IP}} + c_2 U_{\mathrm{harm}}$, where c_1 and c_2 are appropriately chosen coefficients. We stress that the choice of reference system affects only the efficiency of the calculations, and not the final results.

Figure 1 compares our *ab initio* melting curve with experimental results from both DAC and shock measurements. For pressures $P < 200$ GPa covered by DAC, our curve lies ~1,000 K above the values of Boehler[24] and ~500 K above the more recent values of Shen *et al.*[3] (who stress that their values are only a lower bound to T_{m}); our agreement with the Williams *et al.*[25] values is close. Our curve falls significantly below the T_{m} measurements of Yoo *et al.*[26] (however, the difficulties of obtaining temperature in shock experiments are well known) in which temperature was deduced by measuring optical emission, but accords quite closely with the Brown and McQueen[27] value of T_{m} obtained by estimating the shock temperature using thermodynamic calculation. There is theoretical evidence that the Brown–McQueen temperature may be more reliable[12]. Our T_{m} of 6,670 K at the ICB pressure is close to the values inferred from some previous estimates[2,28], and gives evidence against the much higher or lower estimates sometimes proposed[2,25]. The entropy and volume of fusion predicted by our calculations will be reported elsewhere (D.A., G.D.P. and M.J.G., manuscript in preparation).

How reliable is our melting curve? For the given GGA expression for electronic exchange-correlation energy, our exhaustive tests on all sources of technical and statistical error indicate a precision of better than 15 meV per atom on the separate Gibbs free energies of solid and liquid, equating to a precision of 300 K on T_{m}, which is at least as good as current experimental errors. To evaluate the accuracy of GGA itself, we have made detailed comparisons with shock Hugoniot and bulk sound-speed data[27] for both solid and liquid, and we find the same close agreement reported in earlier *ab initio* work[13] on the close-packed solid. Given the accuracy of the *ab initio* low-temperature pressure–volume curve and of phonon frequencies at ambient pressure, we believe that the GGA error in the difference of free energy between solid and liquid is unlikely to be more than 20–30 meV; this implies an error in T_{m} of ~300 K. We therefore believe that our predictions for T_{m} are good to ±600 K. This suggests that they are consistent with the DAC T_{m} values of Williams *et al.*[25] and the lower bounds of Shen *et al.*[3], but not with the melting curve of Boehler[24]; at high pressures, we are consistent with the T_{m} of Brown and McQueen[27], and just within range of the T_{m} of Yoo *et al.*[26].

Light impurities in the Earth's core will shift the temperature at the ICB away from T_{m} for pure Fe. The most likely impurity candidates are sulphur, oxygen, silicon, and perhaps carbon and hydrogen. Apart from our ignorance of the impurity content, the main problem in estimating the ICB temperature is our inadequate knowledge of the thermodynamic properties of solid and liquid alloys of Fe with these impurities at Earth's core conditions. We believe that extension of our *ab initio* techniques will lead to progress here. *Ab initio* thermodynamic integration can be used to calculate the chemical potentials of iron and sulphur in liquid and solid Fe–S alloys as a function of P, T and concentration (D.A. *et al.*, unpublished results). Knowledge of the chemical potentials enables the determination of the separation of a given impurity between solid and liquid phases, and the associated shift of T_{m}.

We have thus presented parameter-free fully *ab initio* calculations of the melting properties of iron in the pressure range 50–350 GPa. The results support some of the experimental measurements of T_{m} over this range, and give a T_{m} value of 6,670 K at the pressure of the inner-core boundary. The *ab initio* techniques for calculating thermodynamic properties under extreme conditions are expected to find application to many other problems concerning the Earth's deep interior. □

Received 6 May; accepted 3 August 1999.

1. Poirier, J. P. *Introduction to the Physics of the Earth's Interior* (Cambridge Univ. Press, 1991).
2. Anderson, O. L. & Duba, A. Experimental melting curve of iron revisited. *J. Geophys. Res.* **102,** 22659–22669 (1997).
3. Shen, G., Mao, H., Hemley, R. J., Duffy, T. S. & Rivers, M. L. Melting and crystal structure of iron at high pressures and temperatures. *Geophys. Res. Lett.* **25,** 373–376 (1998).
4. Belonoshko, A. B. & Ahuja, R. Embedded-atom molecular dynamics study of iron melting. *Phys. Earth Planet. Inter.* **102,** 171–184 (1997).
5. Gillan, M. J. The virtual matter laboratory. *Contemp. Phys.* **38,** 115–134 (1997).
6. Car, R. & Parrinello, M. Unified approach for molecular dynamics and density functional theory. *Phys. Rev. Lett.* **55,** 2471–2474 (1985).
7. Perdew, J. P., Chevary, J. A., Vosko, S. H., Jackson, K. A., Pederson, M. R., Singh, D. J. & Fiolhais, C. Atoms, molecules, solids and surfaces: Applications of the generalized gradient approximation for exchange and correlation. *Phys. Rev. B* **46,** 6671–6687 (1992).
8. Stixrude, L., Cohen, R. E. & Singh, D. J. Iron at high pressure: Linearized-augmented-plane-wave computations in the generalized-gradient approximation. *Phys. Rev. B* **50,** 6442–6445 (1994).
9. Vočadlo, L., Brodholt, J., Alfè, D., Gillan, M. J. & Price, G. D. *Ab initio* free energy calculations on the polymorphs of iron at core conditions. *Phys. Earth Planet. Inter.* (in the press).
10. Söderlind, P., Moriarty, J. A. & Wills, J. M. First-principles theory of iron up to earth-core pressures: Structural, vibrational and elastic properties. *Phys. Rev. B* **53,** 14063–14072 (1996).
11. Vočadlo, L., de Wijs, G. A., Kresse, G., Gillan, M. & Price, G. D. First-principles calculations on crystalline and liquid iron at Earth's core conditions. *Faraday Discuss.* **106,** 205–217 (1997).

12. Wasserman, E., Stixrude, L. & Cohen, R. E. Thermal properties of iron at high pressures and temperatures. *Phys. Rev. B* **53,** 8296–8309 (1996).
13. Stixrude, L., Wasserman, E. & Cohen, R. E. Composition and temperature of the Earth's inner core. *J. Geophys. Res.* **102,** 24729–24739 (1997).
14. de Wijs, G. A. *et al.* The viscosity of liquid iron at the physical conditions of the Earth's core. *Nature* **392,** 805–807 (1998).
15. Alfè, D. & Gillan, M. J. First-principles simulations of liquid Fe–S under Earth's core conditions. *Phys. Rev. B* **58,** 8248–8256 (1998).
16. Alfè, D., Price, G. D. & Gillan, M. J. Oxygen in the Earth's core: A first-principles study. *Phys. Earth Planet. Inter.* **110,** 191–210 (1999).
17. Blöchl, P. E. The projector augmented wave method. *Phys. Rev. B* **50,** 17953–17979 (1994).
18. Kresse, G. & Joubert, D. From ultrasoft pseudopotentials to the projector augmented-wave method. *Phys. Rev. B* **59,** 1758–1775 (1999).
19. Kresse, G. & Furthmüller, J. Efficient iterative schemes for *ab-initio* total-energy calculations using a plane-wave basis set. *Phys. Rev. B* **54,** 11169–11186 (1996).
20. Sugino, O. & Car, R. *Ab-initio* molecular-dynamics study of first-order phase transitions—melting of silicon. *Phys. Rev. Lett.* **74,** 1823–1826 (1995).
21. de Wijs, G. A., Kresse, G. & Gillan, M. J. First-order phase transitions by first-principles free-energy calculations: The melting of Al. *Phys. Rev. B* **57,** 8223–8334 (1998).
22. Kresse, G., Furthmüller, J. & Hafner, J. *Ab-initio* force-constant approach to phonon dispersion relations of diamond and graphite. *Europhys. Lett.* **32,** 729–734 (1995).
23. Frenkel, D. & Smit, B. *Understanding Molecular Simulation* Ch. 4 (Academic, New York, 1996).
24. Boehler, R. Temperature in the Earth's core from melting-point measurements of iron at high static pressures. *Nature* **363,** 534–536 (1993).
25. Williams, Q., Jeanloz, R., Bass, J. D., Svendesen, B. & Ahrens, T. J. The melting curve of iron to 250 gigapascals: A constraint on the temperature at Earth's center. *Science* **286,** 181–182 (1987).
26. Yoo, C. S., Holmes, N. C., Ross, M., Webb, D. J. & Pike, C. Shock temperatures and melting of iron at Earth core conditions. *Phys. Rev. Lett.* **70,** 3931–3934 (1993).
27. Brown, J. M. & McQueen, R. G. Phase transitions, Grüneisen parameter, and elasticity for shocked iron between 77 and 400 GPa. *J. Geophys. Res.* **91,** 7485–7494 (1986).
28. Poirier, J.-P. & Shankland, T. J. Dislocation melting of iron and the temperature of the inner core boundary, revisited. *Geophys. J. Int.* **115,** 147–151 (1993).
29. Andrault, D., Fiquet, G., Kunz, M., Visocekas, F. & Häusermann, D. The orthorhombic structure of iron: An in situ study at high-temperature and high-pressure. *Science* **278,** 831–834 (1997).

Acknowledgements

The calculations were run on the Cray T3E machines at Manchester CSAR Centre and the Edinburgh Parallel Computer Centre. We thank L. Vočadlo for discussions.

Correspondence and requests for materials should be addressed to D.A. (e-mail: d.alfe@ucl.ac.uk).

Stable isotope evidence for the food web consequences of species invasions in lakes

M. Jake Vander Zanden*‡, John M. Casselman† & Joseph B. Rasmussen*

* *Department of Biology, McGill University, 1205 Ave. Dr. Penfield, Montreal, PQ, H3A 1B1, Canada*
† *Science Development Transfer Branch, Ontario Ministry of Natural Resources, Glenora Fisheries Station, RR4, Picton, ON, K0K 2T0, Canada*

Species invasions pose a serious threat to biodiversity and native ecosystems[1,2]; however, predicting and quantifying the impacts of invasive species has proven problematic[3–6]. Here we use stable isotope ratios to document the food-web consequences of the invasion of two non-native predators, smallmouth bass and rock bass, into Canadian lakes. Invaded lakes had lower littoral prey-fish diversity and abundance than uninvaded reference lakes. Consistent with this difference, lake trout from invaded lakes had more negative $\delta^{13}C$ values (−29.2‰ versus −27.4‰) and reduced trophic positions (3.3 versus 3.9) than those from reference lakes, indicating differences in food-web structure. Furthermore, a comparison of the pre- and post-invasion food webs of two recently invaded lakes showed that invasion was followed by substantial declines in littoral prey-fish abundance and the trophic position of lake trout, reflecting a shift in the diet of lake trout towards zooplankton and reduced dependence on littoral fish. This study demonstrates the use of stable isotope techniques to detect changes in food-web structure following perturbations; in this instance, bass-induced food-web shifts may have severe consequences for native species and ecosystems.

Human dominance over the Earth's ecosystems has been accompanied by the widespread introduction of exotic species, which has led to the extinction of native species, the collapse of native fisheries and the loss of ecological integrity and ecosystem functioning[1,7,8]. Ecologists are far from being able to predict, detect or measure the ecological impacts of species invasions[3–6]. This is not surprising because natural food webs are variable and complex[9,10], and using traditional methods to examine the impact of species invasions on aquatic food webs would be laborious, difficult and costly.

Natural stable-isotope distributions are increasingly used to provide a time-integrated measure of food-web relationships based on energy flows. Stable nitrogen isotope ratios ($\delta^{15}N = ({}^{15}N/{}^{14}N_{sample} - {}^{15}N/{}^{14}N_{reference}/{}^{15}N/{}^{14}N_{sample}) \times 1000$) become enriched by 3–4‰ between prey and predator tissues, thereby providing a measure of consumer trophic position[11–13]. Stable carbon isotope ratios ($\delta^{13}C$) exhibit little or no trophic level enrichment (<1‰), and are useful for identifying the sources of production for consumers in lakes because benthic algae are typically enriched in $\delta^{13}C$ relative to phytoplankton[14,15].

Here we use stable isotope techniques to quantify the food-web consequences of recent invasions of smallmouth bass (*Micropterus dolomieu*) and rock bass (*Ambloplites rupestris*) in Canadian lakes. Smallmouth bass have been intentionally introduced (both authorized and unauthorized) into aquatic ecosystems well beyond their native range in North America, and on virtually every continent[16,17]. Furthermore, both bass species may be inadvertently introduced into aquatic ecosystems by the dumping of unused live bait[18], and both are adept at dispersing throughout drainage systems. Consequently, both species have greatly expanded their geographical range over the last century.

These two bass species are presently invading a number of relatively pristine lakes in North America's Northern Hardwood–Boreal Forest transition zone, many of which contain lake trout

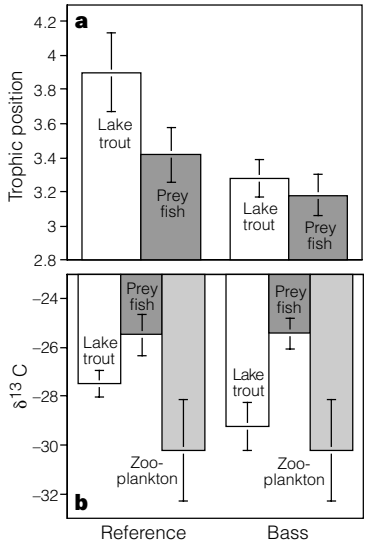

Figure 1 Trophic position and $\delta^{13}C$ values. **a**, Comparison of mean trophic position of lake trout and pelagic forage fish from invaded and reference lakes. **b**, Comparison of mean $\delta^{13}C$ values of lake trout, littoral prey-fish and zooplankton from invaded and reference lakes. Error bars represent 1 s.e.m. using lake-specific averages.

‡ Present address: Department of Environmental Science and Policy, One Shields Avenue, University of California-Davis, Davis, California 95616, USA.